The out-of-equilibrium dynamics of the Sherrington–Kirkpatrick model

2008 J. Phys. A: Math. Theor. 41 324018

(http://iopscience.iop.org/1751-8121/41/32/324018)

IOP PUBLISHING JOURNAL OF PHYSICS A: MATHEMATICAL AND THEORETICAL

J. Phys. A: Math. Theor. **41** (2008) 324018 (17pp) doi:10.1088/1751-8113/41/32/324018

The out-of-equilibrium dynamics of the Sherrington–Kirkpatrick model

Leticia F Cugliandolo[1] **and Jorge Kurchan**[2]

[1] Université Pierre et Marie Curie—Paris VI, Laboratoire de Physique Théorique et Hautes Energies, 4 Place Jussieu, 75252 Paris Cedex 05, France
[2] PMMH, ESPCI rue Vauquelin, 75251 Paris Cedex 05, France

E-mail: leticia@lpthe.jussieu.fr and jorge@pmmh.espci.fr

Received 27 November 2007, in final form 16 March 2008
Published 30 July 2008
Online at stacks.iop.org/JPhysA/41/324018

Abstract
The analytic solution to the dynamics of the Sherrington–Kirkpatrick model was developed in the 1990s. It involves directly measurable out-of-equilibrium quantities, and thus addresses the questions relevant to an experimental system. We here review the out-of-equilibrium relaxation of this model and how it compares to experimental measurements.

PACS numbers: 05.70.Fh, 75.10.Nr, 75.50.Lk

(Some figures in this article are in colour only in the electronic version)

1. Introduction

Most analytic studies of spin-glasses carried out before the early 1990s focused on their Gibbs–Boltzmann measure. The use of the replica trick, the cavity method and the Thouless–Anderson–Palmer (TAP) approach yielded a rather complete description of the equilibrium states of the Sherrington–Kirkpatrick model [1] and other disordered systems. The picture that emerged is one of an extremely complex free-energy landscape with many minima, the lowest of which are the equilibrium 'pure states'. The geometrical organization of these states, and their relative weights in the equilibrium measure are the main objects in the Parisi theory [2], at the centre of which is the disorder averaged functional order parameter $P(q)$ giving the probability that two equilibrium configurations have an overlap q.

A much more difficult programme, not quite completed yet, concerns the understanding of the organization of the landscape away from the equilibrium configurations. Questions such as the metastable state stability, their basins of attraction, and the nature of the barriers separating them, have proven to be much harder to answer in an unambiguous way. This more detailed knowledge of the landscape may seem a necessary condition for the understanding of the experimental, non-equilibrium situation. Surprisingly enough, it turns out that a direct solution of the out-of-equilibrium dynamics is in fact quite simple.

The dynamic approach was pioneered by Sompolinsky and Zippelius in the early 1980s, as a method to avoid the use of replicas for the calculation of equilibrium quantities [3]. They introduced the general framework and succeeded in calculating the high-temperature quantities. The low-temperature situation turned out to be more complicated, and the problem of finding a true dynamic equilibrium solution remains open to this day.

An alternative approach, developed in the early 1990s, is to study the out-of-equilibrium dynamics starting from a quench in temperature, just as in the experimental protocols [4, 5]. Although one might have expected that such a situation is hopelessly difficult, as it involves the landscape far from equilibrium, including the basins of attraction and barriers associated with metastable states, it turns out that the actual analytic solution is only slightly—if at all—harder than the equilibrium one using replicas.

In general, the Gibbs–Boltzmann measure can be explored with a stochastic process that satisfies detailed balance. In order for the system to equilibrate, the limit of large times is taken *before* the thermodynamic limit:

$$\lim_{N\to\infty} \quad \lim_{t\to\infty} . \tag{1}$$

Times are measured after a preparation instant, typically the moment when an instantaneous quench into the high- or low-temperature phase is performed and temperature is henceforth kept constant. The order of limits (1) guarantees ergodicity since barriers can be overcome at sufficiently long times for finite N. The equilibrium thermodynamical values of any operator O are then obtained as the long-time limit of noise averaged time-dependent observables, $\langle O\rangle_{\rm eq} = \lim_{N\to\infty}\lim_{t\to\infty}\langle O(t)\rangle$.

The existence of divergent barriers in spin-glass mean-field models led Sompolinsky [6] to postulate that these systems relax in a set of hierarchically ordered timescales that eventually diverge with N. These N-dependent timescales entered the solution proposed for the saddle-point equations of motion via the time-decay of the correlation and response functions. In this ansatz, although equilibrium was assumed, the fluctuation–dissipation relation between correlation and response was violated. As several authors pointed out, this is clearly inconsistent [2, 7, 8]: the problem can be traced back to the fact that the saddle point dynamic equations are only valid when $N \to \infty$ and the times are kept finite. In any event, both the existence of many timescales and the important role of the fluctuation–dissipation relations were found to be crucial features of the problem that reappeared in later developments.

A different situation, closer to the experimental procedure, is to consider the relaxation of infinite systems at long but finite times using initial conditions that are not correlated with the quenched disorder [4]. The order of limits is then

$$\lim_{t\to\infty} \quad \lim_{N\to\infty} . \tag{2}$$

Divergent barriers in the thermodynamic limit imply ergodicity breaking: the relaxational dynamics does not explore the full phase-space in finite times at large N. In fact, there is no equilibration time $t_{\rm eq}$ such that for all subsequent times the system reaches either the Gibbs–Boltzmann distribution or any time-independent distribution in a fixed, restricted sector of phase space. The dynamics is for all times something different from local equilibrium. This is the phenomenon of *aging*: the relaxation of the system depends on its history at all times. Though aging effects lie beyond the scope of thermodynamics, they have been observed in numerous disordered systems. As we shall see below, the dynamics of mean-field disordered models (2) capture aging phenomena with similarities and differences from what is observed experimentally.

In what follows we summarize what is known about the out-of-equilibrium dynamics of the Sherrington–Kirkpatrick (SK) model [1]. We describe the analytic solution to the relaxational dynamics in the limit (2) [5, 9] and we briefly confront its behaviour to the one observed in experimental systems.

2. The Sherrington–Kirkpatrick (SK) model

The SK Hamiltonian is $H = -\sum_{i<j}^{N} J_{ij} s_i s_j$ where the interaction strength J_{ij} are independent random variables with a Gaussian distribution with zero mean and variance $\left[J_{ij}^2\right] = 1/(2N)$. The square brackets stand for the average over the couplings. The spin variables take values ± 1 [1].

Although the natural dynamics for Ising spin systems are of Glauber [10] or Monte Carlo type, these are not well adapted to implement analytical calculations. It is then preferable to transform the discrete variables into continuous ones and to use Langevin dynamics [3]. The Hamiltonian of the soft-spin SK model is then

$$H = -\sum_{i<j}^{N} J_{ij} s_i s_j + a \sum_i \left(s_i^2 - 1\right)^2 + \frac{1}{N^{r-1}} \sum_{i_1<\cdots<i_r}^{N} f_{i_1\ldots i_r} s_{i_1} \ldots s_{i_r}, \tag{3}$$

$-\infty \leqslant s_i \leqslant \infty, \forall i$. Letting $a \to \infty$ one recovers the Ising case, although this is not essential. Additional source terms ($f_{i_1\ldots i_r}$ time independent) have been included. If $r = 1$ the Zeeman coupling to a local magnetic field f_i is recovered.

The dynamics is given by the Langevin equation

$$\Gamma_0^{-1} \partial_t \sigma_i(t) = -\frac{\delta H}{\delta \sigma_i(t)} + f_i(t) + \xi_i(t). \tag{4}$$

Γ_0 determines the timescale and it is henceforth set to 1. $\xi_i(t)$ is a Gaussian white noise with zero mean and variance $2k_{\mathrm{B}}T$ and we set $k_{\mathrm{B}} = 1$ hereafter. $f_i(t)$ represent any other perturbing force. For example, non-potential forces are important in the analysis of rheological experiments and are mimicked as

$$f_i = \epsilon \sum_{j \neq i} J_{ij}^a s_j \tag{5}$$

with J_{ij}^a being an antisymmetric matrix, $J_{ij}^a = -J_{ji}^a$. Forces that oscillate in time can be used to mimic the slow relaxation under shaking of systems such as granular matter. Such forces maintain the system in a driven out-of-equilibrium regime even if the limit (1) is considered. The mean over the thermal noise is hereafter represented by $\langle \ldots \rangle$.

The dynamics of a Langevin process is usually expressed with a functional integral for the generating functional by using the so-called Martin–Siggia–Rose method. As De Dominicis first pointed out, one does not need to use the replica trick to analyse the relaxation of models with quenched disorder if the initial condition is not correlated with the quenched randomness [11]. The analysis of the relaxational dynamics of a disordered model is thus considerably more straightforward than that of the statics, in particular since all observables have a very clear physical interpretation and can be easily and directly accessed with experiments and numerical simulations.

The sample-averaged dynamics for $N \to \infty$ is entirely described by the evolution of the two-time correlation and the linear response functions [3],

$$C(t,t') \equiv \frac{1}{N} \sum_{i=1}^{N} [\langle s_i(t) s_i(t') \rangle] \qquad R(t,t') \equiv \frac{1}{N} \sum_{i=1}^{N} \left[\left. \frac{\delta \langle s_i(t) \rangle}{\delta f_i(t')} \right|_{f=0} \right].$$

The square brackets denote disorder average. Exact dynamic equations for the evolution of these dynamic macroscopic order parameters, in the *strict* large N limit taken at the outset of the calculation, have been written down by Sompolinsky and Zippelius [3]. They are rather cumbersome because, just as in the static case, the spin variables cannot be explicitly integrated away. Several paths can be followed to approximate the effect of the quartic term introduced by the soft-spin potential. One possibility is to use a mode-coupling approximation [12]. Another possibility is to focus on the dynamics close to the critical temperature, use the fact that the transition is expected to be second order, and deal with the dynamic counterpart of the 'truncated model' introduced by Parisi for the equilibrium case.

All parameters in the resulting large-N equations are independent of N and finite, and have a unique solution. In the high temperature, $T > T_g = 1$, regime the evolution reaches equilibrium, while below T_g this is no longer the case. In the following we focus on the relaxation in the low-temperature phase.

3. Analytic solution

In this section we summarize the analytic solution to the SK model [5].

3.1. Generic properties

The following properties appear to be quite generic of glassy dynamics.

Separation of timescales. After a (long) time t' there is a quick relaxation in a 'short' time-delay $t - t'$ and the self-correlation decays to a value $q_{\rm ea}$, followed by a slower drift away. The parameter $q_{\rm ea}$ is interpreted as the Edwards–Anderson parameter that represents the size of a 'trap' or the 'width of a channel' in phase space. Within these traps the system is fully ergodic while it becomes more and more difficult to escape a trap as time passes. The correlation and response functions can thus be written in a way that explicitly separates the terms corresponding to the relaxation within a trap:

$$C(t,t') = C_{st}(t,t') + C_{\rm ag}(t,t'), \qquad R(t,t') = R_{st}(t,t') + R_{\rm ag}(t,t'). \tag{6}$$

Consistently, $C_{st}(t,t')$ and $R_{st}(t,t')$ are assumed to satisfy the equilibrium relations, i.e. time homogeneity and the fluctuation–dissipation theorem (FDT),

$$\begin{aligned} C_{st}(t,t') &= C_{st}(t-t') \\ R_{st}(t,t') &= R_{st}(t-t') \end{aligned} \qquad R_{st}(t-t') = \theta(t-t')\frac{\partial C_{st}(t-t')}{\partial t'}$$

and

$$\begin{aligned} &C_{st}(0) = 1 - q_{\rm ea}, && \lim_{t-t'\to\infty} C_{st}(t-t') = 0, \\ &C_{\rm ag}(t,t) = q_{\rm ea}, && \lim_{t\to\infty} C_{\rm ag}(t,t') = 0. \end{aligned}$$

Weak ergodicity breaking. The correlation satisfies

$$\frac{\partial C_{\rm ag}(t,t')}{\partial t} \leqslant 0, \qquad \frac{\partial C_{\rm ag}(t,t')}{\partial t'} \geqslant 0. \tag{7}$$

This means that the system, after a given time t', starts drifting away (albeit slowly) until it reaches the maximal distance (in general much larger than the size of a state) at sufficiently long times t.

Weak long-term memory. The integrated linear response satisfies

$$\lim_{t\to\infty} \chi(t,t') \equiv \lim_{t\to\infty} \int_0^{t'} {\rm d}t'' R(t,t'') = 0 \qquad \forall \text{ fixed } t'. \tag{8}$$

$\chi(t, t')$ is the normalized (linear) response at time t to a constant small magnetic field applied from $t'' = 0$ up to $t'' = t'$, often called the 'thermoremanent magnetization'. This hypothesis is crucial, since the response function represents the memory the system has of what happened at previous times: the weakness of the long-term memory implies that the system responds to its past in an averaged way, the details of what takes place during a finite time tend to be washed away (the 'high-school' effect). In interesting cases, the system however does not have only short-term memory

$$\lim_{t\to\infty} \int_0^t \mathrm{d}t' R_{\mathrm{ag}}(t, t') > 0 \tag{9}$$

so that fields acting during an appreciable fraction of the distant past have a finite effect.

3.2. High-frequency 'quasi-equilibrium' dynamics

The Sompolinsky–Zippelius [3] results for the equilibrium dynamics within a pure state can be reinterpreted in the out-of-equilibrium context to describe the first quick relaxation regime. One finds that the self-correlation decays to the plateau at the Edwards–Anderson parameter given by

$$(\tau - q_{\mathrm{ea}}) + q_{\mathrm{ea}}^2 = 0 \qquad \Rightarrow \qquad q_{\mathrm{ea}} = \frac{1 + \sqrt{1 - 4\tau}}{2} \sim 1 - \tau \tag{10}$$

where $\tau = T_g - T$.

$$C_{st}(t, t') \sim A(t - t')^{-a(T)} \tag{11}$$

with $a(T)$ being a nontrivial temperature-dependent exponent.

3.3. Aging regime

The dynamic equations in the aging regime can be solved by using the properties listed above. The slowness of the dynamics allows one to neglect the effect of the time-derivative and write down coupled integral equations for C_{ag} and R_{ag}. These equations are invariant under reparametrizations of time, $t \to h(t)$, that transform the 'fields' C_{ag} and R_{ag} as

$$C_{\mathrm{ag}}(t, t') \to C_{\mathrm{ag}}(h(t), h(t')), \qquad R_{\mathrm{ag}}(t, t') \to \dot{h}(t') R_{\mathrm{ag}}(h(t), h(t')). \tag{12}$$

This invariance deserves some explanation. The complete equations of motion have no such symmetry. However, in the large-time limit, the equations for the 'aging' correlation and responses C_{ag}, R_{ag} become less and less dependent of the timescale, because time-derivative terms become less and less relevant. Only in the infinite time limit are time-derivatives negligible and reparametrizations become a true symmetry.

(Broken) symmetries are related to divergent susceptibilities and large spontaneous fluctuations. Here, these susceptibilities and fluctuations will diverge only in the large-time (or vanishing frequency) limit.

Let us see this with a concrete example [13]. If we add to the equations of motion (4) a forcing term of the form (5), one can show that aging disappears *whatever the value of* ϵ, and correlations become stationary at large times:

$$C_{\mathrm{ag}}(t, t') = \mathcal{C}\left(\frac{\ln(t - t')}{\epsilon}\right). \tag{13}$$

The time for such a stationary regime to be achieved grows with ϵ. Hence, we have that the system has an arbitrarily large susceptibility with respect to the forces f_i (because the two-point correlation functions depend strongly on them), provided we wait long enough.

One can also reason in terms of spontaneous fluctuations, as we shall see below, a path that suggests the introduction of a 'sigma model' that encapsulates the fluctuations in the 'almost-flat' directions [14].

3.4. Correlation scales

The analysis of the aging regime in the SK model motivated the study of generic properties of time correlation functions and the development of a complete classification of their possible behaviour [5].

Take three ordered times $t_3 \geqslant t_2 \geqslant t_1$, and the corresponding correlations are $C(t_i, t_j)$. The monotonicity of the decay of the correlations with respect to the longer time (keeping the shorter time fixed) and the shorter time (keeping the longer time fixed) allows us to derive general properties that strongly constrain the possible scaling forms. Indeed, one can relate any three correlation functions via *triangle relations* [5]

$$\lim_{\substack{t_1\to\infty \\ C(t_2,t_1)=C_{21} \\ C(t_3,t_2)=C_{32}}} C(t_3, t_1) = f(C_{32}, C_{21}), \tag{14}$$

where $f(x, y)$ is a function that determines the form of the triangles whose vertexes are configurations at three large times. The fact that the limit exists is a reasonable working assumption. (Note that we defined f using the correlation between the longest and the intermediate as the first argument.)

The function f is time-reparametrization invariant, associative $f(x, (y, z)) = f((x, y), z))$, it has an identity and a zero, and it is bounded. Exploiting these properties we showed that the most general f is composed of pieces satisfying either of the two forms:

$$f(x, y) = \jmath^{-1}(\jmath(x)\jmath(y)), \qquad \text{isomorphic to the product.} \tag{15}$$

$$f(x, y) = \min(x, y), \qquad \text{ultrametric.} \tag{16}$$

This allows us to classify every possible ansatz. Note that for $\jmath$ equal to the identity the first type of function becomes simply $f(x, y) = xy$, hence the name. It is also possible to prove that the first kind of function (15) is only compatible with the time scaling

$$C(t_2, t_1) = \jmath^{-1}\left(\frac{h(t_2)}{h(t_1)}\right), \tag{17}$$

with $h(t)$ being a monotonically growing function. The dynamics of a given model can occur in two or more correlation scales. In particular, for the SK model

(i) f is isomorphic to the product for correlation values in the stationary regime, $C > q_{\rm ea}$, and $h(t) = \mathrm{e}^{t/\tau}$;
(ii) f is ultrametric for correlation values in the aging regime, $C < q_{\rm ea}$.

Even though dynamic ultrametricity seems mysterious at first sight there is a simple graphical construction that allows one to test it. Take two times $t_3 > t_1$ such that $C(t_3, t_1)$ equals some prescribed value, say $C(t_3, t_1) = 0.3 = C_{31}$. Plot now $C(t_3, t_2)$ against $C(t_2, t_1)$ using $t_2, t_1 \leqslant t_2 \leqslant t_3$, as a parameter. Depending on the value of C_{31} with respect to $q_{\rm ea}$ we find two possible plots. If $C(t_3, t_1) > q_{\rm ea}$, for long enough t_1, the function f becomes isomorphic to the product. Plotting then $C(t_3, t_2)$ for longer and longer t_1, the construction approaches a limit in which $C(t_3, t_2) = \jmath^{-1}(\jmath(C_{31})/\jmath(C(t_2, t_1)))$. If, instead, $C_{31} < q_{\rm ea}$, in the long t_1 limit the construction approaches a different curve.

A preasymptotic scaling that leads to ultrametricity in the limit of diverging times has been found by Bertin and Bouchaud in their study of the dynamics of the critical trap model

[15]. Indeed, it is simple to check that for any three correlations scaling as

$$C(t,t') \sim \frac{\ln(t-t')}{\ln t'} \tag{18}$$

relation (16) is recovered asymptotically.

Ultrametricity in time is also very clear for a driven system satisfying (13). In the limit of small ϵ one can check that $C(t_3-t_1) = \min[C(t_3-t_2), C(t_2-t_1)]$. There is some evidence for it in the 4D Edwards–Anderson (EA) model. In 3D instead the numerical data does not support this scaling [16]. Whether this is due to the short times involved or if the asymptotic scaling is different in 3D is still an open question that will probably never be answered numerically or experimentally, as it was argued in [13] that time ultrametricity would take astronomic times to show up even if present asymptotically.

3.5. Fluctuation–dissipation theorem (FDT)

The analytic solution is such that, in the asymptotic limit in which the waiting-time t_w diverges after $N \to \infty$, the integrated linear response approaches the limit

$$\lim_{\substack{t_w\to\infty \\ C(t,t_w)=C}} \chi(t,t_w) = \chi(C) \tag{19}$$

when t_w and t diverge while keeping the correlation between them fixed to C [5]. Deriving this relation with respect to the waiting time t_w, one finds that the opposite of the inverse of the slope of the curve $\chi(C)$ is a parameter that replaces temperature in the differential form of the FDT. Thus, using equation (6) one defines

$$T_{\rm eff}(C) \equiv -(\chi'(C))^{-1} \tag{20}$$

($k_{\rm B} = 1$), that can be a function of the correlation. Under certain circumstances one can show that this quantity has the properties of a temperature [17].

One of the advantages of this formulation is that, just as in the construction of triangle relations, times have been 'divided away' and relation (6) is invariant under the reparametrizations of time (12). Moreover, the functional form taken by $\chi(C)$ allows one to classify glassy systems into sort of 'universality classes'.

Equation (6) is easy to understand graphically. Let us take a waiting time t_w, say equal to 10 time units after the preparation of the system (by this we mean that the temperature of the environment has been set to T at the initial time) and trace $\chi(t,t_w)$ against $C(t,t_w)$ using t as a parameter (t varies between t_w and infinity). If we choose to work with a correlation that is normalized to one at equal times, the parametric curve starts at the point ($C(t_w,t_w) = 1$, $\chi(t_w,t_w) = 0$) and ends in the point ($C(t\to\infty,t_w) \to 0$, $\chi(t\to\infty,t_w) = \overline{\chi}$). Now, let us choose a longer waiting time, say $t_w = 100$ time units, and reproduce this construction. Equation (6) states that if one repeats this construction for a sufficiently long waiting time, the parametric curve approaches a limit $\chi(C)$.

In the SK model one finds

$$T\chi(C) = \begin{cases} 1-C, & C > q_{\rm ea} \\ 1-q_{\rm ea}+\left(q_{\rm ea}^2 - C^2\right), & C < q_{\rm ea}. \end{cases} \tag{21}$$

This result corresponds to having a succession of temporal scales each one with an effective temperature, $T_{\rm eff}(C)$.

The question as to whether this behaviour strictly applies to the finite-dimensional case remains open. Fluctuation–dissipation violations, i.e. the existence of $T_{\rm eff} \neq T$ in the infinite waiting-time limit, do exist, for instance, in systems with growing domains, but we still have no

examples in which we are certain that $T_{\rm eff}$ stays bounded away both from T and from infinity, in the large waiting-time limit (the latter being the case for coarsening models). Numerical simulations in finite dimensional spin-glass and structural glass models show a clear deviation from FDT during the out-of-equilibrium relaxation but these are obtained for finite times and although these times are relatively long it is hard to extract the truly asymptotic limit.

3.6. Functional dynamic order parameter

In [4] a set of generalized susceptibilities

$$I^r(t) \equiv \lim_{N\to\infty} \frac{r!}{N^r} \sum_{i_1<\ldots<i_r} \left[\frac{\delta \langle s_{i_1}(t)\ldots s_{i_r}(t)\rangle}{\delta f_{i_1\ldots i_r}} \right]_{h=0}$$
$$= r \int_0^t \mathrm{d}t' C^{r-1}(t,t') R(t,t') \tag{22}$$

and their generating function $P_d(q)$

$$1 - \lim_{t\to\infty} \lim_{N\to\infty} \frac{r!}{N^r} \sum_{i_1<\ldots<i_r} \left[\frac{\delta \langle s_{i_1}(t)\ldots s_{i_r}(t)\rangle}{\delta f_{i_1\ldots i_r}} \right]_{h=0} = \int_0^1 \mathrm{d}q' P_d(q') q'^r \tag{23}$$

were introduced. The physical meaning of $P_d(q)$ is clear. If the order of large system size and long time limits are reversed, the generating functional becomes the Parisi static functional order parameter.

The analytic solution of the non-equilibrium dynamics of the SK model is such that $P_d(q) = P(q)$, even if the physical situations that these two-order parameters describe are very different [5]. All generalized susceptibilities converge, then, to the equilibrium values [18]. This result suggests that the landscape the SK dynamics visits at different long times is similar to the one that characterizes the equilibrium pure states (though with finite barriers separating the traps visited dynamically). Although at long but finite times with respect to N the SK model explores regions of phase space that it will eventually leave never to return, some geometrical properties of these regions coincide with those of the equilibrium states.

In other words, the landscape of the model is self-similar in the sense that the dynamics at different (long) times explores entirely different regions of phase-space, and yet the geometry of the trajectories (as characterized by the triangle relations), and the response–correlation relation remain the same. More surprisingly, even if at all finite times the overlap between the current configuration and an equilibrium state is zero, the response–correlation relation in the SK model bears a relation to the equilibrium $P(q)$, although this is not true for all mean-field models.

A similar conclusion was reached in a slightly different context in [9]. The quantities studies there were the staggered auto-correlation and linear response:

$$C(\lambda; t_1, t_2) \equiv \langle \sigma_\lambda(t_1)\sigma_\lambda(t_2)\rangle = \sum_{ij} \langle \lambda|i\rangle\langle\lambda|j\rangle \langle \sigma_i(t_1)\sigma_j(t_2)\rangle, \tag{24}$$

$$R(\lambda; t_1, t_2) \equiv \left\langle \frac{\delta\sigma_\lambda(t_1)}{\delta f_\lambda(t_2)} \right\rangle = \sum_{ij} \langle\lambda|i\rangle\langle\lambda|j\rangle \left\langle \frac{\delta\sigma_i(t_1)}{\delta f_j(t_2)} \right\rangle, \tag{25}$$

where λ denotes the eigenvalues of the $N \times N$ random matrix J_{ij} associated with the eigenvectors $|\lambda\rangle$. $|\sigma(t)\rangle$ is the time-dependent N-dimensional vector of spins, $\sigma_i(t) \equiv \langle i|\sigma(t)\rangle$, and $\sigma_\lambda(t) \equiv \langle\lambda|\sigma(t)\rangle$ are the staggered spin states. We showed that the staggered auto-correlation distribution, $C(\lambda, \mathcal{C})$, between two large and widely separated times t_1 and t_2 chosen

such that $C(t_1, t_2) = \mathcal{C} \leqslant q_{\rm ea}$ coincides with the static one computed with configurations belonging to two equilibrium states with mutual overlap $\mathcal{C}$. Moreover, if one stores the configuration at times t_2 and let the system evolve up to a time t_3 such that again $C(t_2, t_3) = \mathcal{C}$ one obtains the same form for the staggered correlation $C(\lambda, t_2, t_3)$. (Note, however, that due to the system's slowing down, $t_2 - t_1 < t_3 - t_2$ if $\mathcal{C} < q_{\rm ea}$.)

The one-time quantities (e.g. nonlinear susceptibilities and staggered magnetization) derived from the dynamics of the SK model thus coincide with those calculated in equilibrium. This fact, though rather surprising for a mean-field model, has been derived under certain assumptions for finite-dimensional models [37].

At the mean-field level, this coincidence holds for models that do not have a 'threshold' level below which the system cannot penetrate in finite times with respect to N. Examples are, e.g., the SK model and the model of a manifold in a random potential with long-range correlations [18, 19], both having a continuous set of correlation scales and being solved by a full replica symmetry breaking (RSB) scheme at the static level. Instead, there is no reason why the free-energy landscape explored dynamically should resemble the static one in models with a threshold, such as the p-spin spherical model [4] (that is characterized, statically by a one-step level of RSB).

Let us remark that the good agreement between the numerical calculation of $C(\lambda, t, t)$ for large t and the static distribution $C(\lambda)$ (see figure 1) constitutes a rather detailed test of the solution of the out-of-equilibrium dynamics for this model. Further studies of the organization of metastable state and their relevance to the out-of-equilibrium relaxation of the SK model appeared in [20].

3.7. Temperature cycling protocols

A means to study the dynamics in the glassy phase in more detail consists in following the evolution of the sample under a complicated temperature history. The protocols that have been more commonly used include temperature and field cycling within the low-temperature phase [22]. Different types of glasses show rather different responses to the change in external parameters. *Spin*-glasses show the puzzling phenomenon of reinitialization of aging following a decrease in temperature, combined with the recall of the situation attained before the downward jump when the original high temperature is restored. Remarkably, when similar protocols were applied to *structural* glasses, e.g. in dielectric constant measurements of glycerol by Leheny and Nagel, no substantial reinitialization was observed [25]. Experiments in *dipole* glasses display an 'intermediate' behaviour in the sense that a temperature cycling provokes strong asymmetric results, as in spin-glasses, while they also present very strong dependencies on the cooling rate, a property that is not observed in spin-glasses though is very common in structural glasses [26].

Mean-field inspired researchers have interpreted the experimental results of temperature cycling experiments using a hierarchical dynamic picture inspired by the organization of equilibrium states in the Parisi solution of the SK model. In this picture one assumes that spin-glasses have a large number of metastable states that are organized in a hierarchical fashion just like the equilibrium states. It is then proposed that the system is composed of (independent) subsystems whose dynamics is given by the wandering in such a landscape [24]. An average over subsystems has to be invoked in order to obtain smooth results as observed in experiments. Instead, droplet picture [28] oriented researchers found the outcome of the same experiments unequivocal evidence for their favourite theory [23].

The outcome of temperature cycling experiments in spin-glasses can be understood within the dynamic solution of the SK model. Moreover, the reasons why these effects should

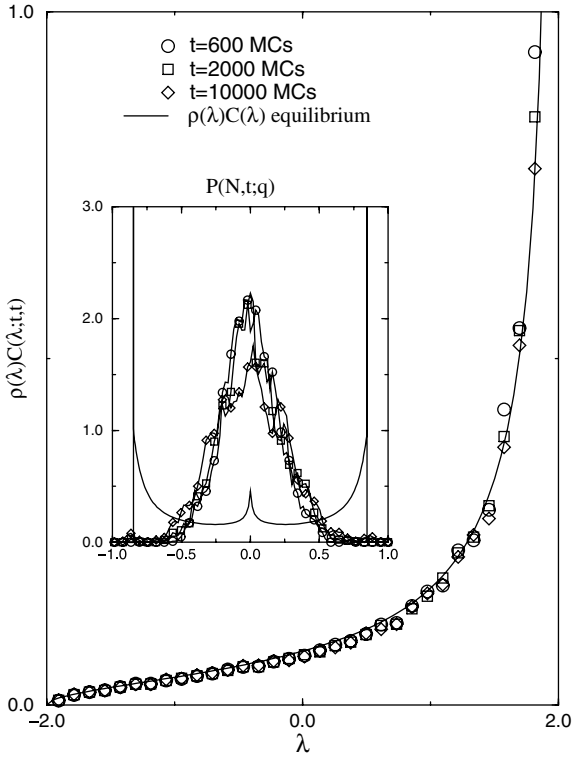

Figure 1. Staggered correlation in the SK model at different times given in the key. $\rho(\lambda)$ is the density of eigenvalues of the interaction matrix J_{ij} that in the large N limit approaches the semi-circle law $\rho(\lambda) = (1/2\pi)\sqrt{2J - \lambda^2}$ for $\lambda \in [-2, 2]$ and zero otherwise, if the variance of J_{ij} is finite. The full line corresponds to the analytic prediction and the points to the numerical Monte Carlo data [9]. Inset: the distribution of the overlap between two copies of the system relaxing from different initial conditions at the same times given in the key. The full line in the inset is the *equilibrium* overlap function $P(q)$ derived by Parisi using the replica calculation with a full replica-symmetry breaking *Ansatz*. The bell-shaped numerical curve demonstrates that the sample is still far from equilibrium. Note that the distribution of the *equal-time* overlaps *is not* the out-of-equilibrium dynamic P_d that does indeed coincide with Parisi's equilibrium P.

be hardly observable in spin-glasses at very short times such as are inevitably involved in simulations, and they are absent in structural glasses are clear within the analytic solution to the dynamics of mean-field models [27].

The key dynamic property to explain the outcome of these experiments is the sharp separation of correlation-scales in the asymptotic waiting-time limit. Take a fixed (but very long) waiting time and let the system evolve further. Imagine at the subsequent time t the self-correlation is $C = q_0 \leqslant q_{\rm ea}$. The decay below this value needs a time-delay that is infinitely longer than $t - t_w$. In other words, at any times t and t_w the correlation (and linear response) can be separated in two terms, a fast and a slow one, such that for all time delays such that $C_{\rm fast}$ changes $C_{\rm slow}$ is fixed while, instead, if $C_{\rm slow}$ varies $C_{\rm fast}$ has reached its limiting value.

The effect of a temperature jump is then very different on the fast and the slow scales. The easiest way to visualize it is to use figure 4(*a*). Upon changing the external temperature the FD plot is modified by changing the slope of the linear part representing the equilibrium FDT

result and, in consequence, the intercept of the line with the curve part that remains unchanged under the Parisi–Toulouse (PaT) hypothesis [35] that consists in two assertions:

(i) $\chi(C)$ is independent of T and H in the aging regime;
(ii) $q_{\rm ea}$ only depends on T and q_0 only depends on H.

The near temperature-independence of $\chi(C)$ in the aging regime of the SK model has been argued at the level of the Parisi static solution and carries through to the non-equilibrium relaxation due to $P_d(q) = P(q)$. It is also a very good approximation in the 4D EA model as checked numerically. As far as we know, there are no tests of this hypothesis in the 3D case.

For temperature T the thin solid line in figure 4(*a*) represents the equilibrium result. In the figure we show the FDT part for a different temperature that we called $T_g(H)$ for the purposes of the discussion of experimental measurements of FDT violations. Here we interpret $T_g(H)$ just as a higher temperature and $q_0(H)$ as its Edwards–Anderson parameter (there is no applied field). For temperature $T_g(H)$ the equilibrium result is the dashed straight line. The thick black curved line is the same at both temperatures. The effect of a temperature change is then quite different on the slow and fast correlation scales. It corresponds to the clockwise or anticlockwise motion of the straight line part of the plot. The slow scales are just modified by a time-parametrization (12), independently of the jump being positive or negative. The scales between q_0 and $q_{\rm ea}$ are instead created or destroyed (restarted or erased) by the negative and positive temperature jumps. This intuitive idea—very close to the one put forward in the hierarchical explanation of temperature jump experiments—can be made precise and implemented in analytic calculations [27].

An argument along the same lines allows one to explain the outcome of field jump experiments.

The phenomenology of structural glasses is described by models of the p-spin type that realize the random first order transition scenario [29]. The aging dynamics of these systems occurs in only one timescale, typically described by a simple t/t_w scaling. In these cases the argument described above does not apply (the decay of the correlation below any value $C < q_{\rm ea}$ is not infinitely slower than the one that occurred before). This yields a theoretical justification of the fact that the outcome of temperature variation experiments in other glassy systems are quite different from the ones in spin-glasses.

3.8. Fluctuations: towards a sigma model approach

Observables in finite-size systems fluctuate. A theory for the disorder-averaged, noise-induced dynamic fluctuations of finite dimensional glassy systems was proposed in [30]. These fluctuations are not induced by the particular realization of quenched disorder but should be generated dynamically in models in which time-parametrization invariance develops asymptotically.

The natural counterpart to the coarse-grained local correlations and responses in finite dimensional models is, for a fully connected model, the global quantity itself. The latter fluctuates if the fully-connected system has a finite size.

One of the main consequences of the time-parametrization invariance theory of fluctuations is that the fluctuations in the fluctuation–dissipation relation in the aging regime should distribute along the global $\chi(C)$ curve. In this subsection we review the analysis of such fluctuations obtained numerically for finite-size SK models.

Finite-size fluctuations of global quantities. If one wishes to show that a given system with a broken symmetry tends to behave like a Sigma model in some limit, what one has to do is to plot the fluctuations of the 'radial' variables that are left invariant by the group, and check

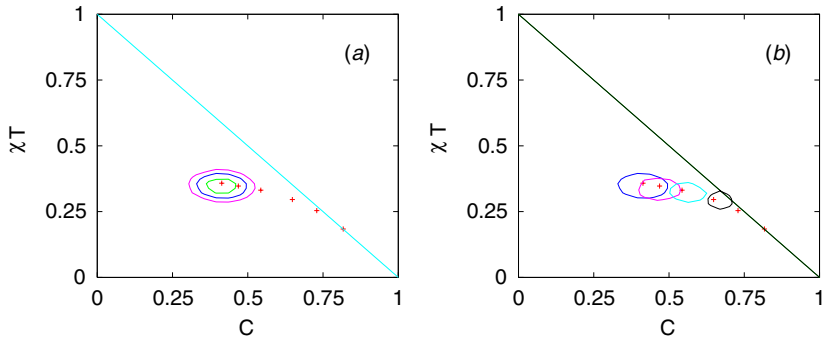

Figure 2. Projection of the joint probability distribution function (PDF) for the global susceptibility and correlations of the SK model with $N = 512$ and $\beta = 2.5$. The strength of the applied field is $\eta = 0.25$. A coarse-graining over time is done using $\tau = 2$ for $t_w = 64$ MCS and $t = 65.70$ MCS, and $\tau_t = 2, 4, 8$ and 16 MCS for $t = 128, 256, 512$ and 1024 MCS. The crosses indicate values averaged over the distribution, the straight line is the prediction from the FDT. In panel (a) the contour levels are chosen at heights corresponding to 95%, 90% and 82% of the maximum in the PDF for the global correlations evaluated at $t_w = 64$ MCS and $t = 1024$ MCS. In panel (b) the contour levels are at 90% of the maximum and they correspond to the PDFs calculated at $t_w = 64$ MCS and $t = 128, 256, 512, 1024$ MCS from right to left. The figure is taken from [31].

that they become vanishingly small compared to those of the 'angular' variables generated by the group itself. In precisely that spirit, in order to show that the system's fluctuations explore preferentially the (almost) flat directions generated by reparametrization invariance, one can plot the fluctuations of correlations and responses in such a way as to show that fluctuations of quantities left invariant by this group (the departures from a χ versus C curve) become negligible with respect to fluctuations generated by reparametrizations (along the χ versus C curve).

Figure 2 shows the level curves of the joint probability of the global susceptibility and correlation of an SK model for a system with $N = 512$ at $T = 0.4$. The distribution functions were obtained using 10^5 pairs $(C(t, t_w), \chi(t, t_w))$ with 10^4 different noise histories, and repeating this procedure with 10 different realizations of disorder. The straight line represents the equilibrium FDT. We see that the probability distribution is peaked on the global $T\chi(C)$ curve. Thus, we conclude that different histories tend to be affected by random time reparametrizations, just as a Sigma model tends to fluctuate along the angles spanned by the group. Very similar results have been obtained in the 3D EA model [31].

Fluctuations in the noise-averaged local quantities. The existence of soft modes for time-parametrization is a feature of slow dynamics, quite independent of the presence of quenched disorder. In order to stress this point, figure 3 shows the distribution over sample realizations of correlations and response function figure 2, the data for each sample being averaged over the noise. The orientation of the contour levels does not follow the $T\chi(C)$ curve but, instead, it is approximately parallel to the FDT straight line. Clearly, the sample-to-sample variations have nothing to do with the reparametrization invariance, which is a dynamic effect. Again, very similar results are obtained in the 3D EA model.

4. Experiments

The SK model is, undoubtedly, the mean-field model of spin-glasses. One would then like to confront its dynamic behaviour to the one observed experimentally. In this section we briefly do this by discussing some salient experimental results.

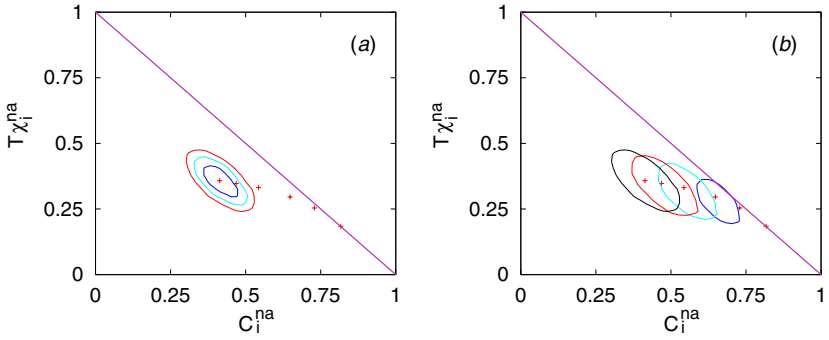

Figure 3. Projection of the joint PDF for the noise-averaged 'local' susceptibilities and correlations of the SK model with $N = 512$ and $\beta = 2.5$. The strength of the applied field is $\eta = 0.125$. The coarse-graining times τ are chosen as in figure 2. The crosses indicate values averaged over the distribution, the straight line is the prediction from the FDT. In panel (a) the contour levels are chosen at heights corresponding to 90%, 85%, 80% and they correspond to times $t_w = 64$ MCS and $t = 1024$ MCS. In panel (b) the contour levels are at 80% and they correspond to the joint PDF at $t_w = 64$ MCS and $t = 1024$ MCS. The figure is taken from [31].

4.1. Isothermal aging

Several groups studied the relaxation of spin-glasses using ac-susceptibility and dc magnetization measurements. The experimental data—as well as the numerical data from simulations of the 3D EA model—are rather well described by a much simpler time dependence than the one found in the SK model. More precisely, neither the ultrametric relation (16) nor its pre-asymptotic form (18) fits the data satisfactorily. Instead, the data are rather accurately described by a two-scale scenario with an aging regime characterized by an enhanced power law, $h(t) \propto e^{\ln^a(t/t_0))}$, with $a \sim 2$, that weakly deviates from a simple power [21]. Note that this scaling is also different from the one predicted by the droplet model [28].

4.2. Temperature cycling experiments

Temperature cycling experiments are amongst the most striking and beautiful ones made with spin-glasses. As mentioned above, the SK model responds to temperature cycling in a manner qualitatively very close to that of experiments. What remains a mystery, however, is that the memory effects in the SK model arise thanks to the existence of many widely-separated timescales, while in the experimental system there seems to be only a single scale.

4.3. Fluctuation–dissipation relation

Direct measurements. Deviations from the FDT should be tested by measuring the dynamic induced and spontaneous fluctuations of a chosen observable using the same experimental device. In a remarkable series of experiments, Hérisson and Ocio carried out such a study focusing on the magnetization of an isolating spin-glass sample [32]. Their results for correlation and linear response functions are compatible with the two-scale scenario and the enhanced power law aging timescale. The direct comparison between integrated linear response and correlation function yields an FD plot that has been interpreted by the authors as being similar to the curved shape of the SK model. It should be stressed, however, that this interpretation is inconsistent with the understanding of the fluctuation–dissipation deviations as being related to the existence of effective temperatures [17], since the whole decay occurs

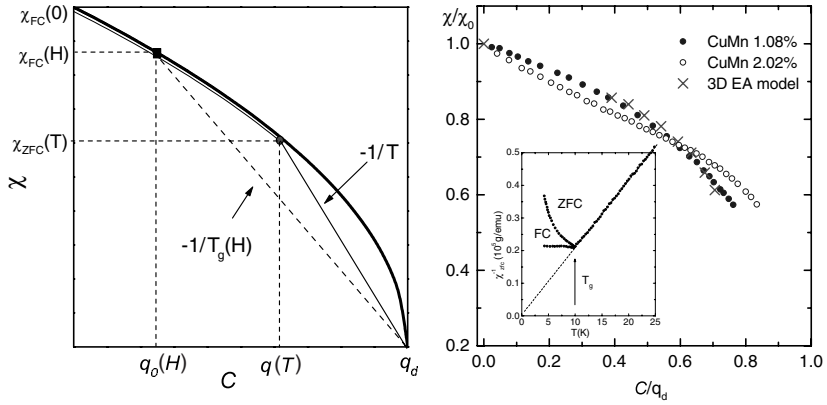

Figure 4. Left: sketch of the χ versus C plot. The thick curve represents the master curve $\chi_{\rm ag}(C)$ that, within the PaT approximation, is temperature and field independent. The thin straight line has slope $-1/T$ ($T < T_g$) and represents equation (26). The dashed straight line has a slope $-1/T_g(H)$ and joins $(q_d, 0)$ to $(\chi_{fc}(H), q_0(H))$. Right: $\chi_{\rm ag}(C)$ plot for CuMn at 1% and 2%. The vertical axis is normalized by the susceptibility at the critical temperature in zero field (χ_0). The horizontal axis is normalized by q_d. The crosses are numerical results for the 3D EA model [36]. The inset shows the inverse FC and ZFC susceptibilities as functions of temperature. The figure is taken from [33].

in a single timescale. Moreover, in our opinion, the resulting FD plot cannot be really distinguished from a broken straight line which is consistent with a two-scale scenario and the effective temperature interpretation. The same *proviso* applies to the numerical data for the 3D EA model.

Zero-field and field-cooled magnetization An indirect study of the fluctuation–dissipation relation using several sets of experimental data obtained from various samples was presented in [33]. The proposal, motivated by discussions with DS Sherrington during a visit to the University of Oxford, is to use the well-known difference between the field-cooled and zero-field cooled magnetization in the low T phase to infer the deviation from the fluctuation–dissipation relation between spontaneous and induced fluctuations.

The approach uses a dynamic extension of the Parisi–Toulouse (PaT) approximation [35] that we explained above. The PaT approximation allows us to estimate the C-dependence of the susceptibility using *exclusively* response results, thus circumventing the difficulties inherent to noise measurements. Deviations from the Curie–Weiss law due to a non-vanishing average of the exchange coupling in real spin-glasses were also taken into account.

The strategy is to use data taken under T and H conditions such that the system is at the limit of validity of FDT, i.e. $C(t, t_w) \sim q_{\rm ea}$. The point $\{q_{\rm ea}, \chi(q_{\rm ea})\}$ is the intersection between the straight part (FDT regime) and the aging part of $\chi(C)$ where

$$\chi(q_{\rm ea}) = \lim_{t-t_w\to\infty} \lim_{t_w\to\infty} \chi(t, t_w) = \frac{1}{T}(q_d - q_{\rm ea}) \tag{26}$$

and to associate $\chi(q_{\rm ea})$ with the zero-field cooled susceptibility $\chi_{\rm zfc}$ is measured experimentally. q_d is the equal time correlation that is not necessarily one but can be obtained from $\lim_{T\to 0} q_{\rm ea}$. The locus of the points obtained by varying T spans a *master curve* $\chi_{\rm ag}(C)$ which, by the PaT hypothesis, is field and temperature independent. At a given working temperature T the actual $\chi(C)$ curve consists of a straight line with slope $-1/T$ joining $(q_d, 0)$ and $(q_{\rm ea}, \chi(q_{\rm ea}))$ and a second part given by $\chi_{\rm ag}(C)$. The method of construction is explained in [33] and it is illustrated in figure 4. A complementary argument uses the

field-cooled magnetization to construct $\chi_{\rm ag}(C)$ by spanning $\chi_{FC}(H) = 1/T_g(H)(q_d - q_0(H))$ as a function of H.

The analysis is most reliable for CuMn, a system in which the Curie–Weiss law as well as the PaT approximation are very well verified. Figure 4 shows the $\chi_{\rm ag}(C)$ curve determined using the ZFC data of Nagata *et al* for two concentrations [34]. There are no experimental points for $C/q_d > 0.8$ that correspond to rather low temperatures. We know, however, that $\chi(C)$ tends to zero as $C \to q_d$ since $\chi_{zfc}(T = 0) = 0$. In addition, the slope $\mathrm{d}\chi/\mathrm{d}C$ should be infinite at $C = q_d$ so that $q = q_d$ only at $T = 0$. The validity of the hypotheses can be judged by the inset where we show the temperature dependence of the inverse susceptibility for the 1.08% compound. A Curie–Weiss law with $\theta \approx 0$ holds accurately for all $T \geqslant T_g$. The T-independence of χ_{fc} required by the PaT approximation is also well verified below the transition. The same is true for the 2.02% sample. For comparison, we also show the curve $\chi(C)$ for the 3D EA model, at $T = 0.7(< T_g)$ and $H = 0$, obtained numerically in [36]. The agreement between the numerical results and the experimental data for the 1.08% sample is remarkable. It may be fortuitous, however, since the results for the 2.02% sample deviate from it. In fact, one must note that $\chi(C)$ is not a universal function. For example, it depends on the details of the Hamiltonian (Heisenberg, Ising and, in general, the level of anisotropy) even at the mean-field level. Thus, there is no reason to expect universality in real systems.

Note that in real samples a spin-glass transition in a field may not exist. However, even if this were the case, the system should remain below a slowly time-dependent *pseudo* de Almeida–Thouless (AT) line for still relatively long times: it ages and behaves as a true (out-of-equilibrium) glass with a non-trivial $\chi(C)$ that would eventually become a straight line with slope $-1/T$.

Another important issue is the asymptotic ($t_w \to \infty$) form of the $\chi_{\rm ag}(C)$ curve. Even if the system never equilibrates, the $\chi_{\rm ag}(C)$ curve may still be a very slowly varying function of t_w, eventually reaching a form different from that observed experimentally. One is not in a position to discard this possibility.

As was mentioned above, equilibrium and large-time non-equilibrium one-time quantities are expected (under certain assumptions) to coincide [37]. If these hypotheses are warranted for spin glasses, the slope of the dynamic $\chi(C)$, for an infinite system in the large-t_w limit should coincide with the static $x(q)$ as defined by the probability of overlaps of configurations taken with the Gibbs measure, the connection being established through the generalized susceptibilities as explained above. The determination of a non-trivial $\chi(C)$ would thus imply a non-trivial $x(q)$ and would hence validate Parisi's solution. The problem, as is usual in these systems, lies in the fact that the dynamics, even in the experimental case, are confined to quite short times.

Numerical experiments have more recently reached timescales almost comparable to the experimental ones. As a consequence, it is now possible to analyse the slow drifts in the field cooled magnetization, and perhaps interpret this in terms of a slowly vanishing Almeida–Thouless line [39].

5. Conclusion

From the dynamic point of view, the Sherrington–Kirkpatrick model has some aspects in which it resembles experimental systems, and some in which it does not. Amongst the resemblances, as we have seen, one can count the fluctuation–dissipation characteristics and the remarkable temperature-cycling properties of memory loss and recovery.

On the other hand, there is the inescapable fact that one does not see any evidence of dynamic ultrametricty either in experimental systems or in their numeric counterparts, while

these are easily observable in simulations of the SK model [38]. Even assuming that at longer times the separation of timescales would develop, this can be estimated to happen not before astronomic times [13].

As mentioned in the previous section, a non-trivial $\chi(C)$ at very long times is an indication of a nontrivial Parisi function. The problem is that experimentally accessible times are not that long—coherence length scales of around 20 are estimated in the best of cases. An apparently nontrivial $\chi(C)$ that would eventually become trivial—or an apparent Almeida–Thouless line disappearing at long times—would be an example of a phenomenon that is a permanent source of confusion: finite-size systems in equilibrium, and infinite-size systems at short times, tend to have a pre-asymptotic behaviour that looks qualitatively mean-field like. This tendency can be judged as positive, because the mean-field picture is then a qualitative model of what we see in practice, or negative, because it does not allow us to distinguish properly between theories.

The Sherrington–Kirkpatrick model was originally designed as a toy model of spin glass, which would serve as a straightforward, practical starting point. Fortunately for us, this expectation proved unfounded, as over 30 years of surprises and amusement have shown.

Acknowledgment

LFC is a member of the Institut Universitaire de France.

References

[1] Sherrington D S and Kirkpatrick S 1975 *Phys. Rev. Lett.* **35** 1792
Kirkpatrick S and Sherrington D S 1978 *Phys. Rev.* B **17** 4384
[2] Mézard M, Parisi G and Virasoro M 1987 *Spin Glass Theory and Beyond* (Singapore: World Scientific)
Fisher K H and Hertz J A 1991 *Spin glasses* (Cambridge: Cambridge University Press)
[3] Sompolinsky H and Zippelius A 1982 *Phys. Rev. Lett.* **45** 359
Sompolinsky H and Zippelius A 1982 *Phys. Rev.* B **25** 6860
[4] Cugliandolo L F and Kurchan J 1993 *Phys. Rev. Lett.* **71** 173
[5] Cugliandolo L F and Kurchan J 1994 *J. Phys. A: Math. Gen.* **27** 5749
[6] Sompolinsky H 1981 *Phys. Rev. Lett.* **47** 935
[7] Houghton A, Jain and Young A P 1983 *Phys. Rev.* B **28** 2630
[8] Franz S and Kurchan J 1992 *Europhys. Lett.* **20** 197
[9] Baldassarri A, Cugliandolo L F, Kurchan J and Parisi G 1995 *J. Phys. A: Math. Gen.* **28** 1831
[10] Szamel G 1997 *J. Phys. A: Math. Gen.* **30** 5727
Szamel G 1998 *J. Phys. A: Math. Gen.* **31** 10045
Szamel G 1998 *J. Phys. A: Math. Gen.* **31** 10053
[11] De Dominicis C 1978 *Phys. Rev.* B **18** 4913
[12] Kennett M P and Chamon C 2001 *Phys. Rev. Lett.* **86** 1622
Kennett M P, Chamon C and Ye J 2001 *Phys. Rev.* B **64** 224408
[13] Barrat J-L, Berthier L and Kurchan J 2001 *Phys. Rev.* E **63** 016105
[14] Chamon C and Cugliandolo L F 2007 *J. Stat. Mech.* 07022
[15] Bertin E and Bouchaud J-P 2002 *J. Phys. A: Math. Gen.* **35** 3039
[16] Picco M, Ricci-Tersenghi F and Ritort F 2001 *Eur. Phys. J.* B **21** 211
[17] Cugliandolo L F, Kurchan J and Peliti L 1997 *Phys. Rev.* E **55** 3898
[18] Franz S and Mézard M 1994 *Europhys. Lett.* **26** 209
[19] Cugliandolo L F and Le Doussal P 1996 *Phys. Rev.* E **53** 1525
Cugliandolo L F, Kurchan J and Le Doussal P 1996 *Phys. Rev. Lett.* **76** 2390
[20] Kurchan J and Laloux L 1996 *J. Phys. A: Math. Gen.* **29** 1929
Biroli G 1999 *J. Phys. A: Math. Gen.* **32** 8365
Biroli G and Kurchan J 2001 *Phys. Rev.* E **64** 016101
[21] Vincent E, Hammann M, Ocio M, Bouchaud J-P and Cugliandolo L F 1997 ed E Rubi (Berlin: Springer) (*Preprint* cond-mat/9607224)

[22] Réfregier P, Vincent E, Hammann J and Ocio M 1987 *J. Phys. (Paris)* **48** 1533
Sandlund L, Svedlindh P, Granberg P, Nordblad P and Lundgren L 1988 *J. Appl. Phys.* **64** 5616
Grandberg P, Lundgren L and Nordblad P 1990 *J. Magn. Magn. Mater.* **92** 228
[23] Nordblad P and Svedlindh P 1998 *Spin Glasses and Random Fields* ed A P Young (Singapore: World Scientific)
[24] Vincent E, Bouchaud J-P, Hammann J and Lefloch F 1995 *Phil. Mag.* B **71** 489
Dupuis V, Bert F, Bouchaud J-P, Hammann J, Ladieu F, Parker D and Vincent E 2005 *Pramana* **64** 1109
[25] Leheny R L and Nagel S R 1998 *Phys. Rev.* B **57** 5154
[26] Alberici-Kious F, Bouchaud J-P, Cugliandolo L F, Doussineau P and Levelut A 1998 *Phys. Rev. Lett.* **81** 4987
Alberici-Kious F, Bouchaud J-P, Cugliandolo L F, Doussineau P and Levelut A 2000 *Phys. Rev.* B **62** 14766
[27] Cugliandolo L F and Kurchan J 1999 *Phys. Rev.* B **60** 922
[28] Fisher D S and Huse D A 1986 *Phys. Rev. Lett.* **56** 1601
[29] Kirkpatrick T R and Thirumalai D 1987 *Phys. Rev. Lett.* **58** 2091
Kirkpatrick T R and Thirumalai D 1987 *Phys. Rev.* B **36** 5388
Kirkpatrick T R and Wolynes P 1987 *Phys. Rev.* A **35** 3072
Kirkpatrick T R and Wolynes P 1987 *Phys. Rev.* B **36** 8552
Kirkpatrick T R, Thirumalai D and Wolynes P 1989 *Phys. Rev.* A **40** 1045
[30] Chamon C, Kennett M P, Castillo H E and Cugliandolo L F 2002 *Phys. Rev. Lett.* **89** 217201
Castillo H E, Chamon C, Cugliandolo L F and Kennett MP 2002 *Phys. Rev. Lett.* **88** 237201
Chamon C, Charbonneau P, Cugliandolo L F, Reichman D R and Sellitto M 2004 *J. Chem. Phys.* **121** 10120
[31] Castillo H E, Chamon C, Cugliandolo L F, Iguain J L and Kennett M P 2003 *Phys. Rev.* B **68** 134442
[32] Hérisson D and Ocio M 2002 *Phys. Rev. Lett.* **88** 257202
Hérisson D and Ocio M 2004 *Eur. Phys. J.* B **40** 283
[33] Cugliandolo L F, Grempel D R, Kurchan J and Vincent E 1999 *Europhys. Lett.* **48** 699
[34] Nagata S, Keesom and Harrison H R 1979 *Phys. Rev.* B **19** 1633
[35] Parisi G and Toulouse G 1980 *J Phys. Lett.* **41** L361
[36] Marinari E, Parisi G, Ricci-Tersenghi F and Ruiz-Lorenzo J J 1998 *J. Phys. A: Math. Gen.* **31** 2611
[37] Franz S, Mezard M, Parisi G and Peliti L 1998 *Phys. Rev. Lett.* **81** 1758
[38] Cugliandolo L F, Kurchan J and Ritort F 1994 *Phys. Rev.* B **49** 6331
Baldassarri A 1998 *Phys. Rev.* E **58** 7047
Takayama H, Yoshino H, Komori T and Hukushima K 1998 *J. Magn. Magn. Mater.* **177** 67
[39] Takayama H and Hukushima K 2007 *J. Phys. Soc. Japan* **76** 013702